Supporting Information

Enquist et al. 10.1073/pnas.0812303106

SI Text

Long-Term Forest Dynamic Plots. The Costa Rican forest was censused in 1976 and 1996. Measurements of woody plant basal stem diameter (diameter at breast height, dbh) were recorded within a permanently marked study plot of seasonally dry tropical forest (10°45′ N, 85°30′ W) within sector Santa Rosa, Area de Conservacíon, Guanacaste (ACG), of northwest Costa Rica (1–3). In 1976, S. P. Hubbell mapped all woody plant stems ≥3 cm dbh (diameter at breast height) within a continuous 680 m × 240 m (16.32 ha) area of forest. Using an identical mapping protocol, Enquist and Enquist completed a second remap of the San Emilio forest 1995 and 1996 by (see ref. 4). In total, 46,833 individuals were surveyed, 26,960 in 1976 and 19,873 in 1996. Together, the two surveys document 20 years of growth and population change within a local community.

The Panamanian Forest, Barro Colorado Island (BCI), was surveyed at ≈5-year intervals starting in 1985. The BCI forest is 50 ha in size and each census includes ≈230,000 individuals. At BCI all stems ≥1 cm dbh were surveyed. Sampling protocols and plot details for this forest are presented in the methods listed in refs. 5–8. The BCI forest data are publically available at http://ctfs.si.edu/datasets/bci/.

The Malaysian forest was censused in 1947 and 1981, allowing a comparison of size structure over an even longer period (34 years) as reported in Manokaran and Kochummen (9). The Malaysian plot is 2.02 ha in area. During the study period, although many of the study species did not show changes in density, eight of the more common species showed significant changes in dominance during this time period (9).

Long-Term Surveys as a Test of the Steady-State Predictions. The multiple-year forest surveys allow comparisons of the size-frequency distributions and nearest neighbor distances across time. Doing so allows us to begin to assess the dynamical nature of our model. In particular, our model predicts that in resource and demographic steady state, the stand-level scaling relationships should remain approximately constant—despite potential changes in species composition. Independence of stand-level exponents across time would be consistent with the resource and demographic steady-state assumptions of our model. Within each of these long-term forest dynamics plots there has been significant turnover in the forest (8, 10). The San Emilio dataset also documented survival and deaths of individual trees over the 20-year period,

The dynamical data for each long-term plot allows for the calculation of the annualized mortality rate as a function of stem radius. For San Emilio, the observed forestwide mortality rate of ≈3% is on the high end for tropical forests (10, 11). Many of the dominant trees have died only to be replaced by species that were of moderate dominance in the community in 1976. More importantly, the turnover observed within the San Emilio forest appears to be driven by a century-long decrease in annual precipitation in Guanacaste. As a likely result the San Emilio forest has seen a significant increase in the dominance of species with more xeric distributions and a decrease in species which are characterized by more mesic distributions (see ref. 10). Thus, for the past 20 years the local community has seen a directional change in species composition and dominance.

Scaling of Mortality Rate. The scaling of mortality rate for BCI and other large 50-ha plots has recently been reported by Muller-Landau et al. (12). The functional form of the mortality functions for several 50-ha forests reported by Muller-Landau et al. is similar to what we report for the San Emilio forest. In addition, for increasingly larger trees, they also report an increasing variance above the predicted mortality function. It would be instructive for the BCI forest, and the other long-term dynamic plots reported in Muller-Landau et al., to generate predictions for the mortality function based on allometric growth data, as we have done here for the San Emilio forest. Mortality data for the Malaysian forest were reported by Manokaran and Kochummen (9). They concluded that mortality rate was independent of tree size class. However, the authors binned the diameter data by using large bins (10-cm increments) and their smallest tree size was 10 cm dbh. As a result, the mortality scaling relationship is crude and it is difficult to assess their data against ours. However, the scaling relationship between tree diameter and annualized mortality rate for similar southeast Asian forests are reported by Muller-Landau et al. (12) and they appear to support the general functional form predicted by our model. Again, it would be instructive to calculate the predicted scaling mortality function based on the growth rate data for this and other forests.

Succession Data. Data from a successional sere of forest plots have been assembled from Sorenson (13). The dataset consists of 13 patches of forest differing in successional age in Sector Santa Rosa, Area de Conservacíon Guanacaste, Costa Rica. Each patch was homogenous in its age and on average was 0.53 km^2 in area (range, 0.30–0.76). Although patch areas varied, all patches were connected with other similarly aged forests and were close to mature forests for seed sources (13). A 600-m transect was surveyed within each of the 13 sites along a random compass bearing with the restriction that the transect must remain within the forest patch. The stem diameter of all individuals within 10 m of either side of the transect were measured, and their species identified. Because of likely measurement error associated with the transect method only stems >5 cm dbh were analyzed in this study. A total of 14.5 ha of forest was sampled.

Plant Allometry and Regression Statistics. The relationship between stem diameter, tree height, and canopy radius was measured for 151 individuals, ranging from saplings to emergent trees, and included 38 of the more dominant species in the forest. Measurements were made by B.J.E. within the San Emilio forest in Guanacaste Costa Rica during the summer of 1999. Height, h_k, was calculated by trigonometry. Canopy radius, r_k^{can}, was measured from the center of the stem out to an average canopy distance. Because there is likely measurement error in both the x and y axes, regression parameters were estimated by using model II or reduced major axis (RMA) regression.

Calculation of the Size Distribution Exponent. For all of our tree plot datasets, except for the Malaysian plot, we calculated the size distribution exponent by using the maximum likelihood estimation (see refs.12, 14–16). Given a random sample of n observations $X_1, \ldots, X_n$, the classical Pareto distribution is defined by

$$S(x) = \Pr\{X \geq x\} = \left(\frac{x}{\omega}\right)^{-a}, \quad x \geq \omega \qquad \text{[S1]}$$

where X represents any one of $X_1, \ldots, X_n$. The value of ω is a normalization that is chosen to reflect a common value across the datasets being studied. In our case ω is the size of the smallest tree used in each dataset. As discussed by Clark et al. (15) and

White et al. (16) the maximum likelihood estimator (MLE) of α, assuming that the value of ω is known, is

$$\alpha_{\mathrm{MLE}} = \frac{n}{\sum Y_i} \qquad \text{[S2]}$$

where $Y_i = \ln(X_i/\omega)$ and again ω is the diameter of the smallest tree in the dataset of interest. For the San Emilio, BCI, and Guanacaste Succession plots α_{MLE} was calculated by using ω = 3 cm dbh, 1 cm dbh, and 5 cm dbh (see above), respectively. The values of ω for the San Emilio and BCI forests were chosen because these were the minimum size cutoffs for these forest surveys.

In the case of the Malaysian dataset, where only binned data are reported, we used simple regression statistics. Statistical tests were conducted by using OLS regression and the 95% confidence intervals for both the slope and intercepts calculated.

To visualize the size distribution for each forest, following Enquist and Niklas (17), size distribution data for San Emilio and BCI were binned at 2-cm-dbh and 1-cm-dbh intervals, respectively. Data from Malaysia, however, were reported by the original authors as binned data. As a result we present their binned data here.

Nearest Neighbor Distance Calculation and Annualized Mortality. Nearest neighbor distance was calculated by using a C++ program finding the nearest neighbor Euclidian distance for each individual within a given size class and then taking an average distance value (and 95% confidence interval) for each size class or bin k. Distances between each stem within a given size class, k, were calculated by using the x, y coordinates recorded for each stem. The C++ program (neartest.cpp), is available on request.

Annualized mortality rates were calculated for the San Emilio forest only for stems that were tagged in 1976 and or were >10 cm dbh in 1976 (4). Because of the lower sample sizes of large tagged trees, annualized mortality rates statistical analysis was only completed on size classes ≥10 individuals.

Additional Equations for Subsection: Predicting Stand Limiting Resource Supply, Stand Energetics, Flux, and Mortality. ***Total stand biomass, total number of individuals, and average tree size.*** Building on the work of Kerkhoff and Enquist (18) and in the light of our theory, from the main text, given Eqs. **9** and **10**, we can show how the total phytomass, M_{Tot}, of the stand is influenced by the size distribution and the allometry of plant form. Specifically,

$$M_{\mathrm{Tot}} = \int m(r)f(r)dr = \int \frac{1}{c_m} r^{8/3} \frac{c_n}{r^2} dr$$

$$= \frac{c_n}{c_m} \int r^{2/3} dr = \frac{3}{5} \frac{c_n}{c_m} r_m^{5/3} \qquad \text{[S3]}$$

where r_m is the radius of the trunk or stem of the largest tree. From Eq. **S3,** the total biomass of the stand increases to the 5/3 power of the size of the largest tree in the stand. Again, the above relations stem from the metabolic rate of an individual $B = b_0 r^2$, where b_0 is a normalization constant, the size distribution function $f(r) = c_n r^{-2}$, where c_n is a normalization constant, and the allometry between stem radius and above-ground biomass $r(m) = c_m m^{3/8}$, where c_m is another normalization constant. Consequently, the total number of individuals within the stand,

$$N_{\mathrm{Tot}} = \int_{r_0}^{r_m} f(r)dr = c_n(r_0^{-1} - r_m^{-1}) \approx c_n/r_0 \qquad \text{[S4]}$$

where r_m is the radius of the largest trunk and r_0 is the radius of the smallest trunk. Similarly, the average size of a tree is

$$\bar{m} \equiv M_{\mathrm{Tot}}/N_{\mathrm{Tot}} \approx (3/5)(1/c_m) r_0 r_m^{5/3} \qquad \text{[S5]}$$

and is influenced by the sizes of the largest and smallest tree.

Environmental and energetic influence on the maximum size of a tree. The maximum size of a tree, r_m will be influenced by several variables, but most importantly by the rate of limiting resource, $\dot{R}$, supply and rate of tree metabolism as

$$r_m \leq \frac{\dot{R}}{(b_0 c_n)} \qquad \text{[S6]}$$

So, the maximum size of a plant or tree is influenced by rate of limiting resource supply, $\dot{R}$, the metabolic rate normalization, b_0 (again, a measure of the metabolic intensity of cells and tissue), as c_n is the size corrected measure of the density of individuals of a given size as $c_n = (dn/dr)/r^{-2}$. In principle, one could measure these quantities. Thus, if c_n and b_0 are similar across sites, then the maximum size of trees will increase with increases in $\dot{R}$, as generally observed.

Total energy or resource or carbon flux of a stand. Again, building on the insights of Kerkhoff and Enquist (18), the total flux of energy (and resources such as carbon, water, and nutrients) within a stand is

$$B_{\mathrm{tot}} = \int B(r)f(r)dr = b_0 c_n \int dr = b_0 c_n [r_m - r_0] \approx b_0 c_n r_m, \qquad \text{[S7]}$$

where $B(r) = b_0 r^2$. Note, linking B_{Tot} to other resources such as carbon would involve knowing the stoichiometric conversion between rates of metabolism and rates of carbon flux. Given Eq. **S3**, the above relationships allow us to give a prediction for how the total flux of energy (and resources such as carbon, water, and nutrients) must scale with the total biomass of the stand so that,

$$B_{\mathrm{Tot}} = b_0 c_n \left(\frac{5 c_m}{3 c_n} M_{\mathrm{Tot}} \right)^{3/5} \qquad \text{[S8]}$$

Ultimately, according to Eq. **S8**, the total flux of resources through the stand is governed by the size distribution of individuals within a forest and the allometric scaling relationships that characterize metabolism and plant form. Approximate support for this prediction may be given by a recent study by Kerkhoff and Enquist (18), which showed that the total net biomass production of vegetation, across a broad range of vegetation types ranging from grasslands to forests, scaled with the 0.46 (95% CI = 0.37–0.56) power of total biomass, which is close to the predicted value of 3/5 or 0.60.

Caveats on the sensitivity of the above predictions to the largest trees. It is important to note that because of the r^2 law for energy use and the r^{-2} law for the number of stems, the total energy use B_{Tot} (discussed in the main text) as well as the total biomass of the stand, M_{Tot}, as detailed in Eq. **S3** will be very sensitive to the contributions of the few largest trees (i.e., the value of r_m). Hence, predictions for B_{Tot} and M_{Tot} will be subject to sizeable sampling error, unless the size of the forest plot is very large, and to additional sources of mortality not specified by our model that may disproportionately influence the largest trees. For example, if there are fewer large trees than predicted by our model (see *Discussion*) then Eqs. **S3**–**S8** will overestimate B_{Tot}, M_{Tot}, N_{Tot}, and $\bar{m}$. As a result, a more accurate estimate of B_{Tot} and M_{Tot} is to sum the values of B_k and M_k across size classes. Nonetheless, our theoretical predictions for B_{Tot} and M_{Tot} are useful because they provide a framework for

quantitatively linking how specific physiological and functional attributes of trees and forests, as well as the importance of rate of limiting resource supply, $\dot{R}$, mechanistically influence stand and ecosystem level properties.

1. Janzen DH (1986) *Guanacaste National Park: Tropical Education, and Cultural Restoration* (Editorial Univ. Estatal a Distancia, San José, Costa Rica), p 104.
2. Janzen DH (1987) Forest Restoration in Costa-Rica. *Science* 235:15–16.
3. Janzen DH (1987) How to grow a tropical national-park: Basic philosophy for guanacaste national-park; northwestern Costa-Rica. *Experientia* 43:1037–1038.
4. Enquist BJ, et al. (1999) Allometric scaling of production and life-history variation in vascular plants. *Nature* 401:907–911.
5. Condit R (1998) *Tropical Forest Census Plots* (Springer, Berlin).
6. Hubbell SP, Foster RB (1992) Short-term dynamics of a neotropical forest: Why ecological research matters to tropical conservation and management. *Oikos* 63:48–61.
7. Harms KE, et al. (2001) Habitat associations of trees and shrubs in a 50-ha neotropical forest plot. *J Ecol* 89:947–959.
8. Condit R, Hubbell SP, Foster RB (1996) Changes in Tree species abundance in a neotropical forest : Impact of climate-change. *J Trop Ecol*12:231–256.
9. Manokaran N, Kochummen KM (1987) Recruitment, growth and mortality of tree species in a lowland dipterocarp forest in Peninsular Malaysia. *J Trop Ecol* 3:315–330.
10. Enquist CAF (2002) Long term changes in a tropical forest. PhD thesis (University of New Mexico, Albuquerque, NM), p 230.
11. Stephenson NL, van Mantgem PJ (2005) Forest turnover rates follow global and regional patterns of productivity. *Ecol Lett* 8:524–531.
12. Muller-Landau HC, et al. (2006) Testing metabolic ecology theory for allometric scaling of tree size, growth and mortality in tropical forests. *Ecol Lett* 9:575–588.
13. Sorensen TC (1998) Tropical dry forest regeneration and its influence on three species of Costa Rican monkeys. Master's thesis (University of Calgary, Alberta, Canada).
14. Clauset A, Shalizi CR, Newman MEJ (2007) Power-law distributions in empirical data. arXiv:0706.1062v1 [physics.data-an].
15. Clark RM, Cox SJD, Laslett GM (1999) Generalizations of power-law distributions applicable to sampled fault-trace lengths: Model choice, parameter estimation and caveats. *Geophys J Int* 136:357–372.
16. White EP, Enquist BJ, Green JL (2008) On estimating the exponent of power-law frequency distributions. *Ecology* 89:905–912.
17. Enquist BJ, Niklas KJ (2001) Invariant scaling relations across tree-dominated communities. *Nature* 410:655–660.
18. Kerkhoff AJ, Enquist BJ (2006) Ecosystem allometry: the scaling of nutrient stocks and primary productivity across plant communities. *Ecol Lett* 9:419–427.

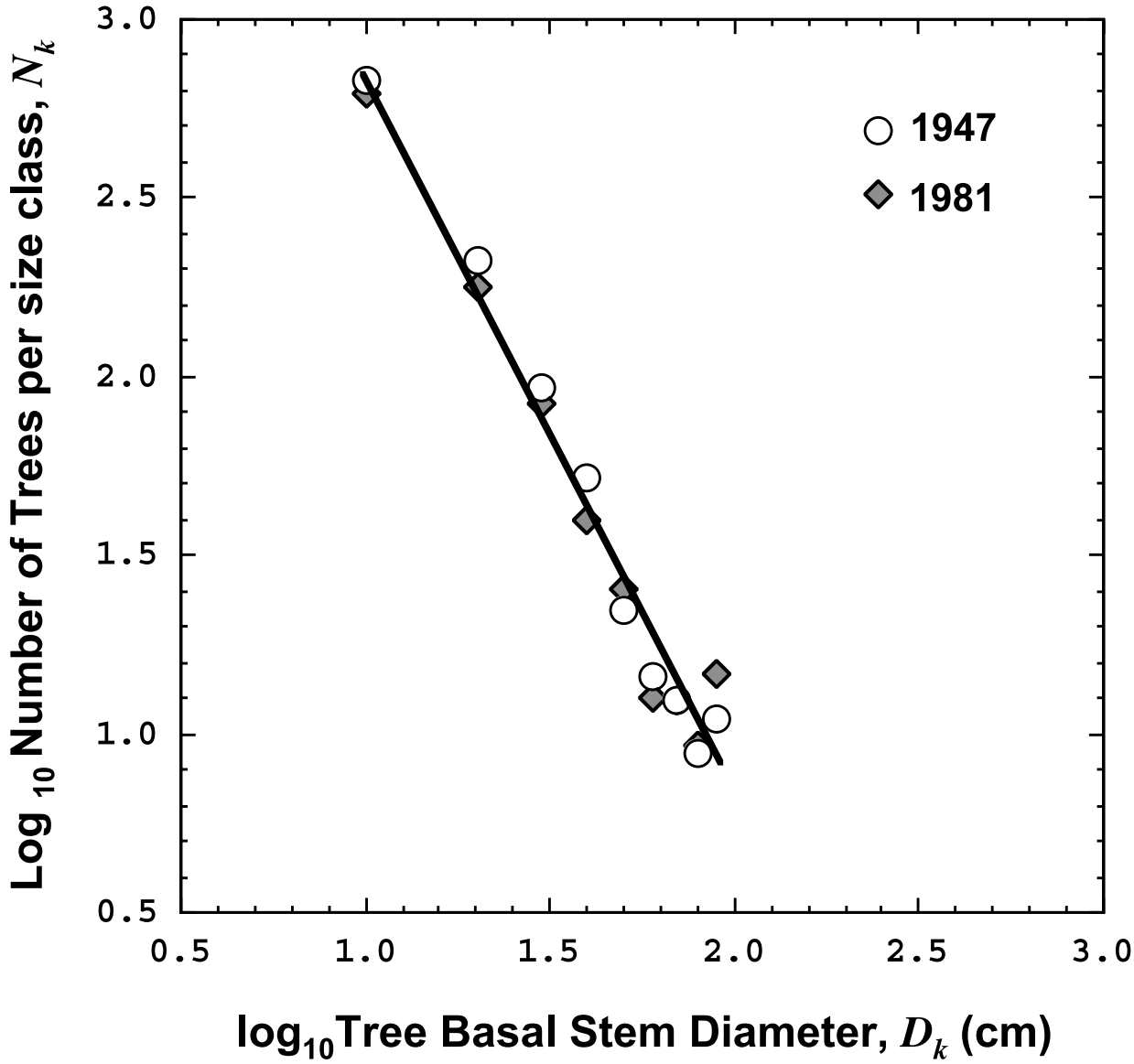

Fig. S1. The size distribution for a ≈2-ha Dipterocarp tropical forest plot in the Sungei Menyala Forest Reserve, Peninsular Malaysia. Two forest surveys in 1947 and 1981 are shown. Data are from Manokaran and Kochummen (9). Again, consistent with the resource and demographic steady-state assumptions of our model, the size distribution exponent does not appear to appreciably change across years despite significant turnover.

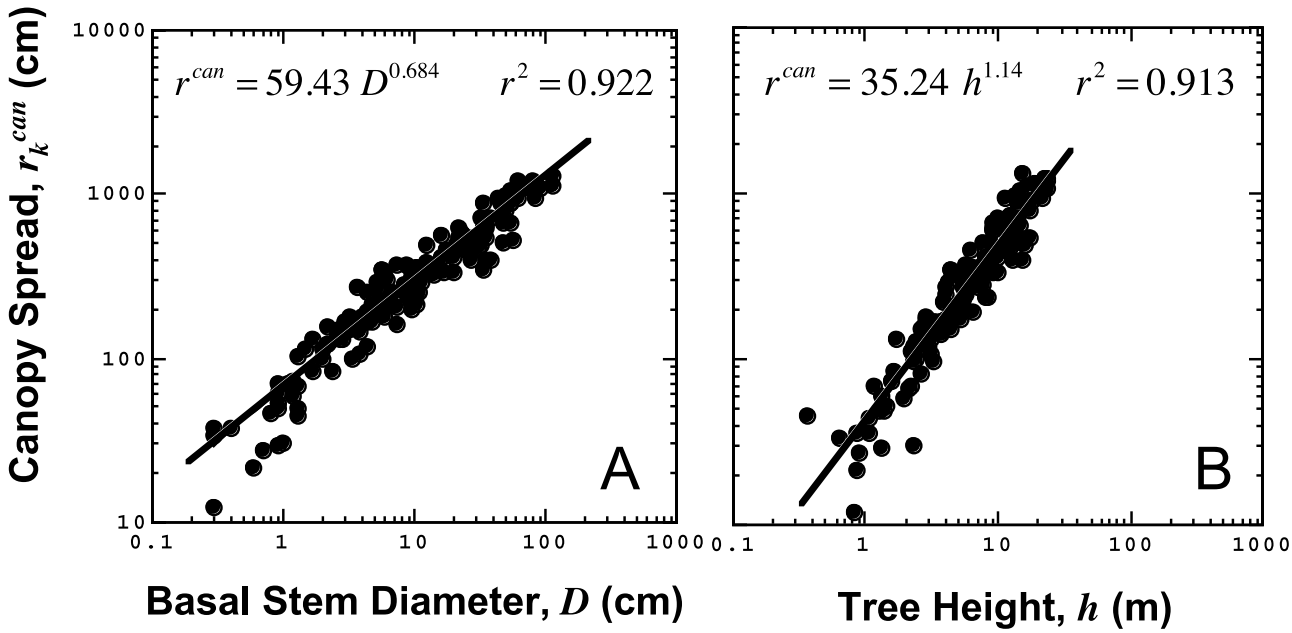

Fig. S2. Scaling of tree canopy dimensions for a random sample of 151 individuals, ranging from saplings to emergent trees, in the San Emilio forest. The data included 38 species. (*A*) A plot of the canopy radius, r_k^{can}, versus basal stem diameter, D_k. The reduced major axis (RMA) regression fit to the data yields an exponent of 0.684 (95% CI = 0.6457–0.7195), indistinguishable from the predicted value of 2/3. (*B*) A plot of the canopy radius, r_k^{can}, versus tree height, h_k. The fitted (RMA) regression yields an exponent of 1.14 (95% CI = 1.08–1.19), very close to the predicted value of 1.0.

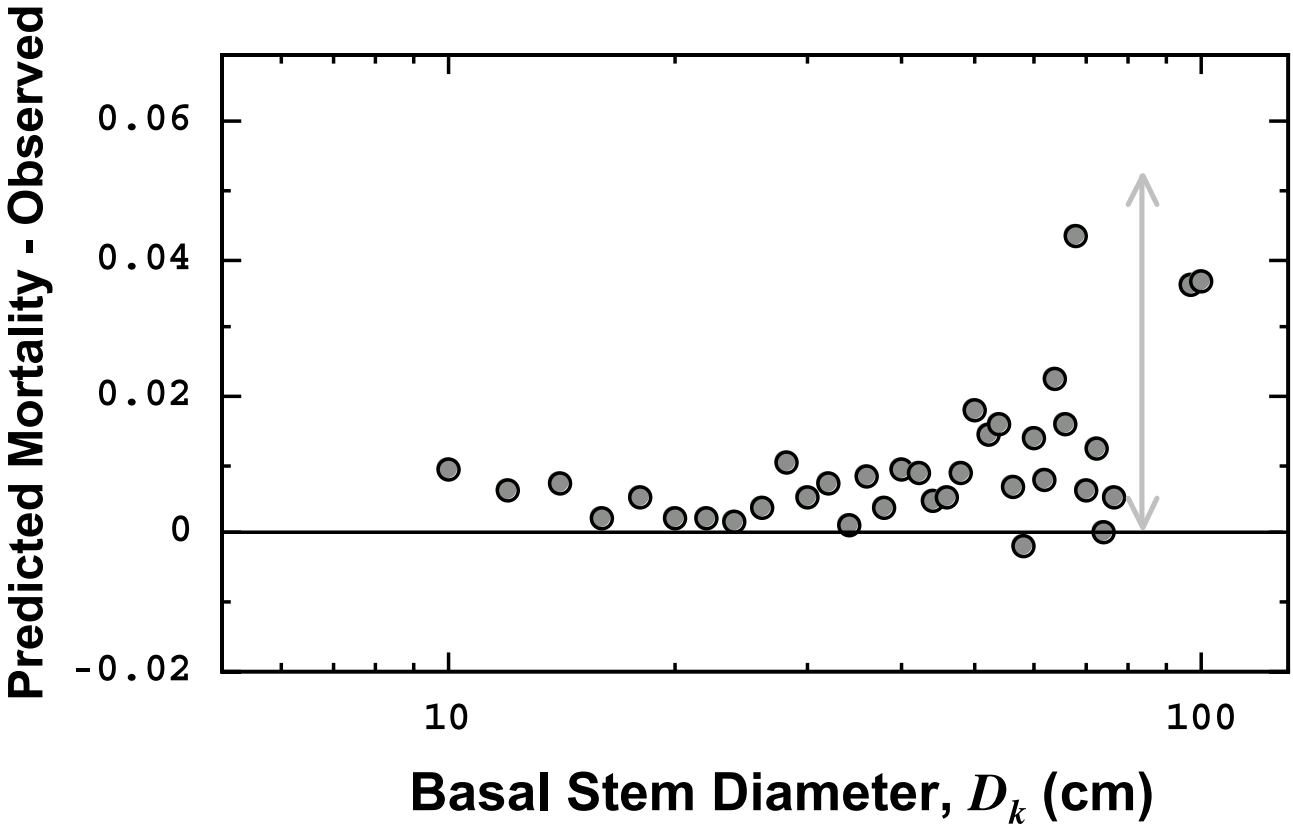

Fig. S3. Plot of the difference between the predicted mortality rate and the observed mortality rate for each size class in the San Emilio Forest, Costa Rica. Points falling close to the horizontal line at zero indicate close correspondence between the predicted mortality rate from our model with observed rates. Data points falling close to the zero line would indicate that all of the observed mortality in that size class is due to competition. However, the data show that, with increasing tree size, there is an increased deviation (see the light-gray arrow) from the mortality expected from steady state. This deviation is consistent with the expectation that additional sources of mortality are increasingly more prevalent for the largest-size classes. Nonetheless, our model provides then a basis to begin to quantify the magnitude of noncompetitively induced mortality.

Table S1. Scaling exponents for the size distribution and nearest neighbor distance for repeated censuses of two tropical forest plots

Forest dynamics plot	Census year	MLE size distribution exponent	OLS nearest neighbor scaling exponent	NND r^2
BCI	1982	−2.079	1.047	0.990
BCI	1985	−2.099	1.039	0.992
BCI	1990	−1.968	1.041	0.989
BCI	1995	−1.940	1.038	0.988
SE	1976	−2.411	0.993	0.983
SE	1996	−2.077	1.044	0.957

Each of these plots was surveyed at different times (see Census year column). For each year of census we calculated the exponent for the size distribution based on the maximum likelihood estimate (MLE) for a power-function. The size distribution exponent is calculated using the MLE. The scaling of nearest neighbor distance was calculated by binning all individuals at 1-cm intervals and then calculating the mean nearest neighbor distance (NND) for that size class; 95% confidence intervals for the mean NND are shown for each size class. Ordinary least squared (OLS) regression was used to fit the scaling of NND data. The fitted exponents for both forest plots (BCI and SE) are generally supportive of the −2 prediction for the size distribution and 1.0 for NND scaling. BCI, Barro Colorado Island, Panama; SE, San Emilio forest, Area de Conservacion, Guanacaste, Costa Rica.